Path Processing and Block Adjustment With RADARSAT-1 SAR Images♥

Thierry TOUTIN
Natural Resources Canada, Canada Centre for Remote Sensing
588, Booth Street, Ottawa, Ontario, K1A 0Y7, Canada
Tel: (613) 947-1293/Fax: (613) 947-1385/thierry.toutin@ccrs.nrcan.gc.ca

Abstract- The objectives of this research study was to determine the conditions of experimentation and application of path processing and block adjustment with synthetic aperture radar (SAR) images when few control is available. The path and block processing enabled the simultaneous adjustment of all images together to reduce the control point requirement. The method is based on the three-dimensional physical model developed for multisensor images at the Canada Centre for Remote Sensing, Natural Resources Canada. These processes were applied to fifteen RADARSAT-1 SAR fine mode images (five paths by three rows) acquired over the Rocky Mountains, Canada from different look angles (F1 and F4) with a weak intersection geometry (6°-angle). The first results of the least squares block adjustment showed that the same errors were obtained with image paths or block (20 m for 3-image paths and 5-path block) as with a single image (18 m). In addition to ground control points (GCPs), elevation tie points (ETPs), with a known elevation value, were used in the overlaps because the 6° look-angle difference of overlapping paths was small. However when using only GCPs in the outer paths for block adjustments, the error results deteriorated from 25 m in both directions for the 3-path block to 270 m in X-direction for the 5-path block. This deterioration was a combination of the image pointing and cartographic errors of GCPs (25-30 m) and the weak 6°-intersection angle. Consequently, GCP distribution every two paths was the solution with this dataset, and better results (35 m) was then achieved using a reduced number of GCPs in the outer paths (25 or even 10 GCPs) and middle path (six GCPs) and 20 ETPs in each overlap. However, the combined image pointing and cartographic errors of GCPs (25-30 m) are included in these 35-m error results and the internal accuracy of the block should thus be better (around one resolution). Finally, the same minimum requirement of GCPs, as a function of their accuracy and the overlap intersection geometry, can be applied for an image, a path or a block.

Index Terms- Block adjustment, error propagation, geometric evaluation, path processing, RADARSAT-1.

I. INTRODUCTION

As in photogrammetry where strips and blocks of aerial photos are processed together, the same process can be applied with satellite images from the same and/or adjacent orbits, thus performing the geometric processing with a block adjustment instead of a single image adjustment, when no sufficient ground control is available. There are different advantages to the block adjustment:

- Number of ground control points (GCPs) can be reduced;

♥ Published in IEEE-TGARS, vol. 41, no. 10, pp. 2320-2328, October 2003.

- Better relative accuracy between the images can be obtained;
- More homogeneous and accurate mosaic over large areas can be obtained; and
- Homogeneous GCP network for geometric processing can be densified or generated.

In the 1960-1970's, the same methods were applied to airborne radar images, but generally obtained with paper films in a manual process. Successful mapping projects over cloud-covered tropical areas produced conventional image map products at scale of 1:250,00 in the form of so-called "semi-controlled" mosaics from airborne radar images and strips [1], [2]. However, the accuracy could be in the range of hundreds of metres. More recently, large area mosaics were generated using European Remote Sensing 1 (ERS-1) synthetic aperture radar (SAR) imagery [3] or RADARSAT-1 SAR imagery [4] with accuracy in the order of 50-100 m. The first study used a full block triangulation process while the second only used a path processing method. While mathematical development for interferometric block parameter adjustment for the Shuttle Radar Topographic Mission [5] or algorithm development for block adjustment of multisensor radar images [6] were addressed, no results and evaluation were presented. Even if block adjustments were applied with RADARSAT-1 to create mosaic over large continents (Australia, Antarctica), to our knowledge few scientific results or applications were published.

This paper will further investigate the path/block adjustment method with RADARSAT-1 SAR images, and mainly evaluate the conditions of the experimentation in order to reduce the control point requirement. The processing of different paths and blocks of 15 images acquired over the Canadian Rocky Mountains using different numbers and distributions of GCPs are addressed. Result comparisons enabled the accuracy of the system and its stability to be evaluated. The mathematical tool used is the geometric correction model developed for SAR images [7] and adapted to RADARSAT-1 SAR images [8] at the Canada Centre for Remote Sensing (CCRS), Natural Resources Canada. An iterative least squares process using ground control and orbit information is used for the block adjustment to simultaneously compute geometric-model parameters of all images and paths.

II. STUDY SITE AND DATA SET

The study site is located in the south of the Canadian Rocky Mountains (British Columbia) (49° N to 50° N; 121° W to 123° W) from Vancouver in the southwest to Okanagan Range in the southeast (Fig. 1). This area is characterized by a rugged topography where elevation ranges from 0-4000 m with a mean slope of a little more than 10° and less than 2% of total slopes more than 35°. The land cover consists mainly of a mixture of coniferous and deciduous trees with patches of agricultural land and clearcut areas, while the mountains over 2500 m are covered by snow and glaciers. The agricultural fields are found mostly along valleys, while the clearcut areas, linked by new logging roads, are distributed over the whole area. Roads are mainly loose or stabilised surface roads in the mountains, and hard surface roads in the valleys. Lakes and ponds are also found which are connected through a series of creeks flowing between steep cliffs.

The topographic data, obtained from the Centre for Topographic Information Sherbrooke, Canada were 42 1:50 000 maps, which have a positioning accuracy of 25-30 m. Even if these paper maps, which are only used for the GCP collection, are not very accurate when compared to the fine mode RADARSAT-1 SAR resolution (8-9 m), they are the most common and sometimes the "only" cartographic source around the world to cover such large area used in a block adjustment project. The digitized 10-m contour lines of maps

are first grouped and used to generate a triangular irregular network, which is then transformed into a 20-m grid file. Break lines and hydrographic features are also added in the topographic DEM processing. The vertical accuracy of the topographic DEM is evaluated to be around 10-15 m.

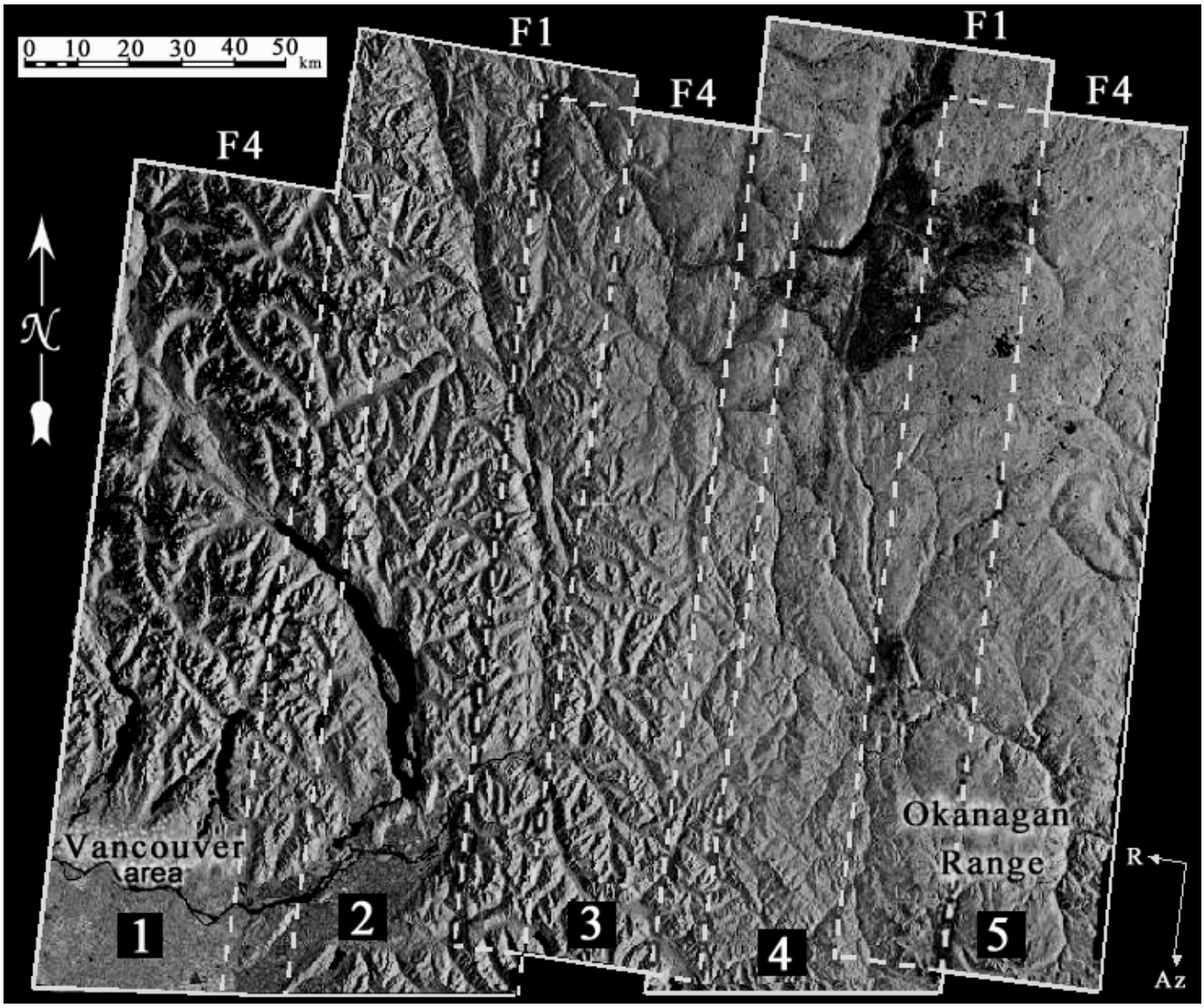

Figure1: RADARSAT-SAR fine mode image paths (50 km by 150 km) and block (200 km by 150 km) acquired from descending orbits over the Canadian Rocky Mountains study site: Vancouver area at the South-West and the Okanagan Range at the South-East

Fifteen RADARSAT-SAR fine mode images were acquired over the study site (Fig. 1 and Table I), and cover an area of 200 km by 150 km. They were alternatively acquired from beam 1 (paths 2 and 4) and beam 4 (paths 1, 3 and 5) from descending orbits because there was no or few overlap between beams 1 and 5. In addition, the choice of fine mode beams with shallow look angles enabled to reduce or even cancel foreshortening, layover and shadows in mountainous areas for slopes less than 37° [9]. The images generated a block of five paths and three rows with approximately 20% overlap between adjacent paths (Fig. 1). With same-side look angles F2-F4 adjacent paths had a weak intersection angle (6°) and

geometry in the overlaps. Since each image path was acquired at the same date from the same physical orbit, the three images of the same orbit were directly processed by RADARSAT International (RSI), Canada to generate 50 5 150 km image path (about 8000 columns 5 24 000 to 28 000 lines). They are in ground range presentation (ellipsoid projection without relief correction), orbit oriented, 6.25-m pixel spacing, coded in 16 bits without any radiometric processing (RSI SGF format).

Table I: Description of RADARSAT-SAR fine mode images paths (50 5150 km) acquired over the Canadian Rocky Mountains study site

SAR Mode & Beam	**Fine, beam 1**	**Fine, beam 4**
Path numbers	2 & 4	1, 3 & 5
Acquisition	06/08/00	02/07/00,
Dates	13/08/00	20/08/00, 03/08/00
Orbit	Descending	Descending
Resolution	9.1 m x 8.4 m	8.1 m x 8.4 m
Image pixel spacing	6.25 m x 6.25.m	6.25 m x 6.25.m
Look angles	37° - 40°	43° - 46°

III. EXPERIMENT

A. Three-Dimensional CCRS Physical Model

The three-dimensional (3-D) CCRS physical model was developed as an integrated and unified geometric modeling to geometrically process SAR images [7], and has also benefited from theoretical work in celestial mechanics to better determine the satellite's osculatory parameters over long orbit. The model was subsequently adapted to RADARSAT imagery [8], [9].

The integration and the derivation of the equations, mainly based on radargrammetry, is out of scope of this paper, but the final results for SAR images, which link the 3-D cartographic coordinates to the image coordinates is given by [7]:

$$Pp + y\,(1 + \delta\gamma X) - \tau h = 0 \qquad (1)$$

$$X + \theta\, h/\cos\chi + \alpha q(Q + \theta X - h/\cos\chi) = 0 \qquad (2)$$

where $$X = (x - ay)(1 + h/N_o) + by^2 + cxy + \delta h h^2 \qquad (3)$$

Each parameter is given using a mathematical formula that represents the physical realities of the full viewing geometry (satellite, sensor, Earth, map projection):

N_o	is the normal distance to the ellipsoid;
a	is mainly a function of the non-perpendicularity of axes;
α	is the field-of-view for an image pixel;
p, q	are the image coordinates;
P, Q	are the scale factors in along-track and across-track directions, respectively;
τ and θ	are a function of the leveling angles in along-track and across-track directions, respectively;

x, y and h	are the 3-D ground coordinates;
b, c, χ, $\delta\gamma$, and δh	are 2nd-order parameters, which are functions of the total geometry, e.g., satellite, sensor, image and Earth.

The images are SAR standard products generally available to users. They are generated digitally during post processing from the raw signal SAR data (Doppler frequency, time delay). Errors present in the input parameters to image geometry model will propagate through to the image data [10]. These include errors in the estimation of slant range and of Doppler frequency and also errors due to the satellite's ephemeris data and the ellipsoid. Assuming the presence of some geometric error residuals, the parameters of the geometric correction model reflect these residuals. Each of these parameters is in fact the combination of several correlated variables of the viewing geometry, so that the number of unknown parameters has been reduced to an independent uncorrelated set. The unknowns parameters are thus translations (in X and Y) and a rotation related to the cartographic North, the scale factors and the levelling angles in both directions, the nonperpendiculatity of axes, as well as some of the second-order parameters when the orbital data are not accurate, such as with RADARSAT-1.

This 3-D physical model has been applied to radar data (ERS, JERS, SIR-C and RADARSAT), as well as visible and infra-red (VIR) data (Landsat-5 and Landsat-7, SPOT-1-5, IRS, ASTER, KOMPSAT, EROS, IKONOS and QuickBird) with three to six GCPs. This 3-D physical model applied to different image types is robust and not sensitive to GCP distribution as soon as there is no extrapolation in planimetry and elevation [7], [9]. Based on good quality GCPs, the accuracy of this model is within one resolution cell for radar images, one-third of a pixel for medium-resolution VIR images and one pixel for high-resolution images.

B. The processing steps

RADARSAT-1 SAR image paths were directly processed by RSI, Canada, and blocks of image paths can be thus generated from paths in the east-west direction acquired from adjacent orbits. In the overlaps between adjacent paths (Fig. 1), tie points (TPs) (i.e., features present in both paths) should be used to link adjacent paths and to increase the relative accuracy between paths. When the intersection angles, as being the difference of the two SAR look angles, between adjacent paths were less than 8° generating weak intersection geometry [11], elevation tie points (ETPs) with known elevation value should be used in the overlaps to strength the intersection geometry between the two adjacent paths and the Earth. In addition, some TPs could be added. After the block was formed, there were three main processing steps for the block adjustments, which are more and less the same than for processing one image:

(1) Acquisition and preprocessing of the RADARSAT-SAR image paths and metadata to determine orbit osculatory parameters and approximate values for each parameter of 3-D SAR physical models;
(2) Collection of ground points with two-dimensional (2-D) image and 3-D cartographic coordinates, of TPs with 2-D image coordinates and ETPs with 2-D image and elevation coordinates. The cartographic coordinates are extracted from the 1:50 000 topographic maps with an accuracy of 25-30 m in planimetry and 10 m in elevation. Fifty to 80 ground points per path were collected, which cover the full elevation range in order to avoid extrapolation not only in planimetry but also in elevation. In fact, there were a total of 167 and 88 GCPs belonging to only one path and two adjacent paths, respectively (Fig. 2). These points were mainly roads with one- to two-pixel (10 to 15 m) image pointing error in the lowest relief and mainly lakes and rivers with two- to three-pixel (15 to 20 m) image pointing error in the highest relief;

(3) Computation of the block adjustment initialized with the approximate parameter values and refined by an iterative least squares adjustment with the GCPs/ETPs/TPs and orbital constraints. Each image point for a GCP contributed to two error equations, and each TP or ETP belonging to two images contributed to one or two error equation(s), respectively. In the block adjustment, GCPs belonging to more than one path were also considered as TPs to create a mathematical link in the error equations between adjacent paths. All points, with fixed coordinates for GCPs and ETPs, were weighted as a function of their accuracy (cartographic and image coordinates) to set up the normal equations, which were resolved with a conventional Cholesky's inversion process. GCP residuals and Independent Check Points (ICPs) errors, as being the differences between the "true" cartographic coordinates and the computed cartographic coordinates, were thus computed for each image/path point. Points in the overlaps belonging to more than one path have thus two error vectors.

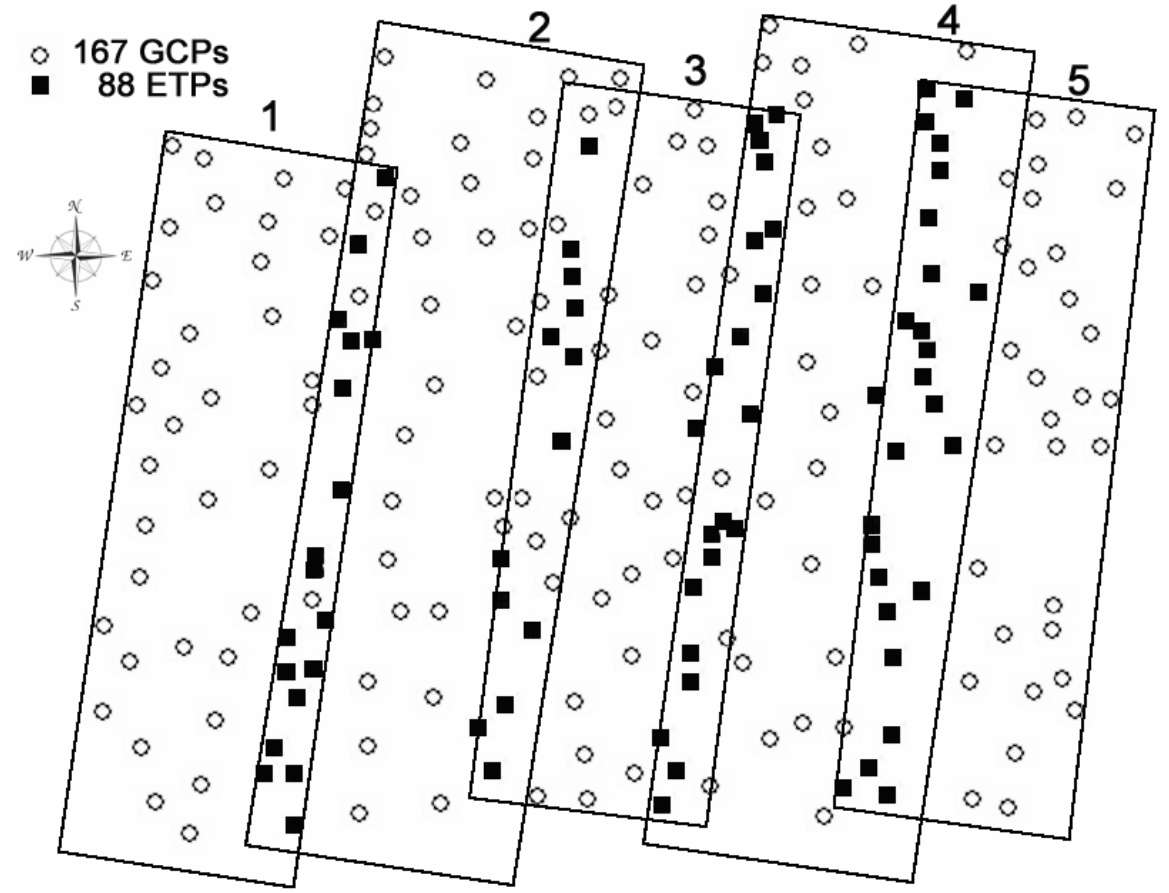

Figure 2: Distribution of 167 GCPs (white circles) and 88 ETPs (black squares) in the RADARSAT-SAR block

Although six accurate GCPs are enough to determine the 3-D physical model of each RADARSAT-SAR image or path, a larger number of points enabled the impact of 25-30 m map errors and 10-20 m image pointing errors in the least squares adjustment computation of 3-D physical models to be reduced or even cancelled due to a large degree of freedom. Accuracy tests with ICPs can also be performed.

C. The path/block adjustment tests

Four sets of path/block adjustments were performed with this dataset by varying the number of paths in

the block and the distribution and number of GCPs used in the adjustment:

A. All points are used as GCPs for a single image (as reference), for the five paths formed with three images ("three-image path") and for the block formed with five paths ("five-path block").
B. Limited number of GCPs for the three-image path processing.
C. All GCPs on the outer images and ETPs in each overlap for three -, four- and five-path blocks.
D. GCPs every two paths ("*checkerboard*") and ETPs in each overlap for the five-path block.

One of major advantages of three-image paths is that the processing request three times less GCPs and processing than three independent images, and the reduction factor is proportional to the number of images in the path. The results on one independent image in Test A were used as reference for comparison with the path/block adjustment results. Test B with different GCP/ICP configurations were used to evaluate for Test D the optimal reduced number of GCPs necessary in the block adjustment in relation to the error of the input data and the overlap intersection geometry.

IV RESULTS

A. All points as GCPs

Table II gives the root mean square (RMS) and absolute maximum residuals (in meters) of the seven different tests where all GCPs were used in the least squares adjustment of: one independent image, the five three-image paths, the five-path block. The results for one independent image, which correspond to the mean results of the 15 independent images, were used as reference for comparison of the other strip/block bundle adjustment results. With the 3-D physical model, the residuals do not reflect the modelling accuracy but rather the error of the input data when there are more GCPs than the minimum required [8], and with a very large number of GCPs RMS residuals/errors from the least squares adjustment will be close from the input data errors. In fact, Table II shows that the RMS residuals are slightly smaller than the GCP planimetric accuracy (image pointing and map).

Table II: Number of GCPs and their RMS residuals (RMS-R) and maximum residuals (Max-R) for the image/path/block adjustments using all GCPs

Image/Path/Block Configuration	**Number of GCPs**	**RMS-R X (m)**	**RMS-R Y (m)**	**Max-R X (m)**	**Max-R Y (m)**
Reference image[a]	27	18	16	37	36
Path 1	54	17	17	38	43
Path 2	80	25	19	49	46
Path 3	75	25	19	45	39
Path 4	72	19	19	42	37
Path 5	62	19	18	40	47
5-path block	343[b]	21	18	48	47

[a] Being the mean of results of 15 images computed separately
[b] GCPs belonging to two paths were counted twice

All path and block tests gave approximately the same results than the reference test with one image: more and less 20 and 18 m in *X* and *Y* axes, respectively with minimum/maximum residuals less than three times the RMS residuals. Because these residuals included the 25- to 30-m map errors of GCPs, the internal accuracy of all path/block adjustments is thus better (in the range of SAR resolution) and these

results were then consistent with previous results (10-m accuracy) [8], [9]. Although non-significant, the RMS residuals for the paths 2 and 3 were worse because these paths mostly covered mountains and GCP image pointing errors were larger. These errors of paths 2 and 3 were also reflected, but less, in the results of the block adjustment. These coherent results (equivalent RMS and maxima) demonstrate the applicability of the geometric model and of the path/block processing with RADARSAT-SAR images, but also show a good stability and robustness of the method without systematic and random errors, regardless of the image/path/block. The use of overabundant GCPs (six is the theoretical minimum per image or path) in the least squares adjustment reduced or even cancelled the propagation of different input data errors (image pointing and cartographic) in the 3-D physical model(s), but conversely these input errors are reflected in the residuals. It is thus normal and "safe" to obtain residuals on the same order of magnitude as the GCP error, but the 3-D physical model(s) will be more accurate because the input error did not propagate into the model(s).

B. A limited number of GCPs for the path processing

The path processing corresponds to the processing of long strips of images (path) acquired from the same orbit and processed without GCP in the path center. The reduction of GCPs is proportional to the number of images in the path. Firstly, different tests were performed by varying the number of GCPs to find the optimal number of GCPs to be used in the path/block adjustments in relation to their errors (image pointing and cartographic) and the same-side weak intersection geometry of this experiment. Since unbiased validation of the positioning accuracy has to be realized with independent data, points not used as GCPs were used as ICPs to verify the model error. Fig. 3 gives the RMS *X*-*Y* residuals (in meters, dashed lines) for the least squares adjustment of path 4 when GCPs varied from 15 to 55, as well as the RMS X-Y errors (in meters, plain lines) for the ICPs varying from 57 to 17, respectively. The maximum variations of ICP RMS errors (plain lines) were only 2 m (20 m to 22 m) in *X*-direction and 6 m (18 m to 24 m) for *Y*-direction. Except for the 15-GCP adjustment, the RMS-error variations (*Y*-variation decreases to 4 m) were not very significant and the geometric model is then not sensitive to GCP number. In addition, these results were similar to those obtained with the previous set of tests (Table I). Consequently, 20-25 GCPs, taking thus the statistical advantage of their overabundance in the least squares adjustment, are the good compromise for this dataset (GCPs and SAR images) to avoid the propagation of 25-30 m errors of GCPs in the block modeling. As mentioned before in Test A, the internal accuracy of the path is better (around one resolution) than the 20-m RMS errors because the cartographic errors of ICPs are included in the error evaluation. However, this 20-25 GCP requirement can be carefully applied to other dataset, and the more accurate is the input data and/or the stronger is the intersection geometry in the overlaps (F1-F5 or S3-S7), the less GCPs is required.

This result of 20-25 GCPs was then applied for path processing using only ten GCPs at North and South ends of each path and no control in the middle. The path processing results were evaluated on RMS errors on the remaining ICPs: they were around 20 m in both axes for paths 1, 4 and 5 and around 25 m and 22 m in *X* and *Y* axes for paths 2 and 3 with maximum errors less than three times the RMS errors (about the same order of magnitude than the previous results in Tests A and B). These results confirmed the adaptability and stability of the 3-D SAR physical model for path processing. While 20-25 GCPs might seem excessive, their collection from 1:50 000 maps was straightforward (taking about 1 h), mainly due to the fact that the image pointing does not need to be more accurate than 1-3 pixels, because the 25-30 m cartographic error is the dominant error in the error budget.

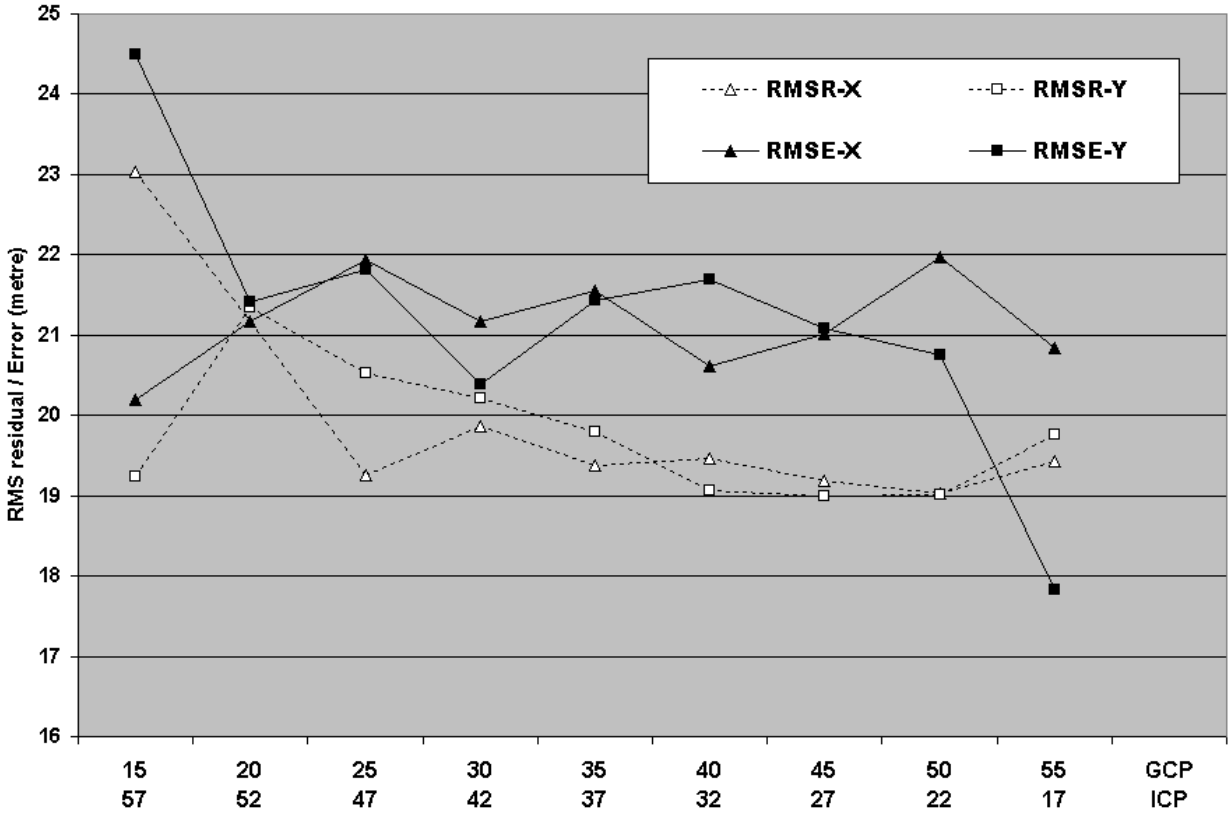

Figure 3: RMS *X*-*Y* residuals (in meters, dashed lines) for the least squares adjustment of path 4 when GCPs varied from 15 to 55, and the RMS *X*-*Y* errors (in meters, plain lines) for the ICPs varying from 57 to 17, respectively.

C. All GCPs on outer paths of blocks

Three blocks were tested: with three, four and five paths. ETPs were used in each path overlap to create a link between outer and inner paths. The adjustment results are checked on the remaining ICPs in the inner paths. Table III gives the number of ICPs and their RMS errors (RMS-E) for the three block adjustments and Fig. 4 shows the results for 3-path block adjustment: the left window with the GCPs (white circles) and ETPs (black squares) distribution and the right window with the ICP error vectors. The image paths with plain lines are the images with GCPs. ICP vectors are the differences between the known and the computed cartographic coordinates for each path point. ICPs belonging to more than one path have thus an error vector for each path: the closer are these error vectors, the smaller is the relative error between the different path points projected on the ground and the better is the superposition of the overlapping paths. The evaluation on these points is then an indication of how good the block bundle adjustment performed.

When there is only one inner path without GCP (three-path block) the results are good (Fig. 4) and of the same order of magnitude as the previous results: approximately 25 m in both axes. However the results, mainly RMS-E in *X*-direction, quickly degraded as soon as the number of inner paths without GCP increased: 65 m and 271 m in *X*-direction for four- and five-path block, respectively. Since the *X*-direction mainly corresponds to the elevation distortion and adjacent paths have same-side weak intersection geometry (6°-angle) the input data error propagated more in *X*-direction and the information is not correctly "transferred" with ETPs from outer paths to inner paths. Since three-path block gave good results with this data set (weak

intersection geometry and poor GCPs), the solution for the five-path block was to use GCPs every two paths ("*checkerboard*").

Table III: Number of ICPs and their RMS errors (RMS-E) for the block adjustments with three to five paths using all GCPs in the outer paths and ETPs in each overlap

Block Configuration	Number of ICPs	RMS-E X (m)	RMS-E Y (m)
3-path block	119	26	24
4-path block	193	65	23
5-path block	293	271	43

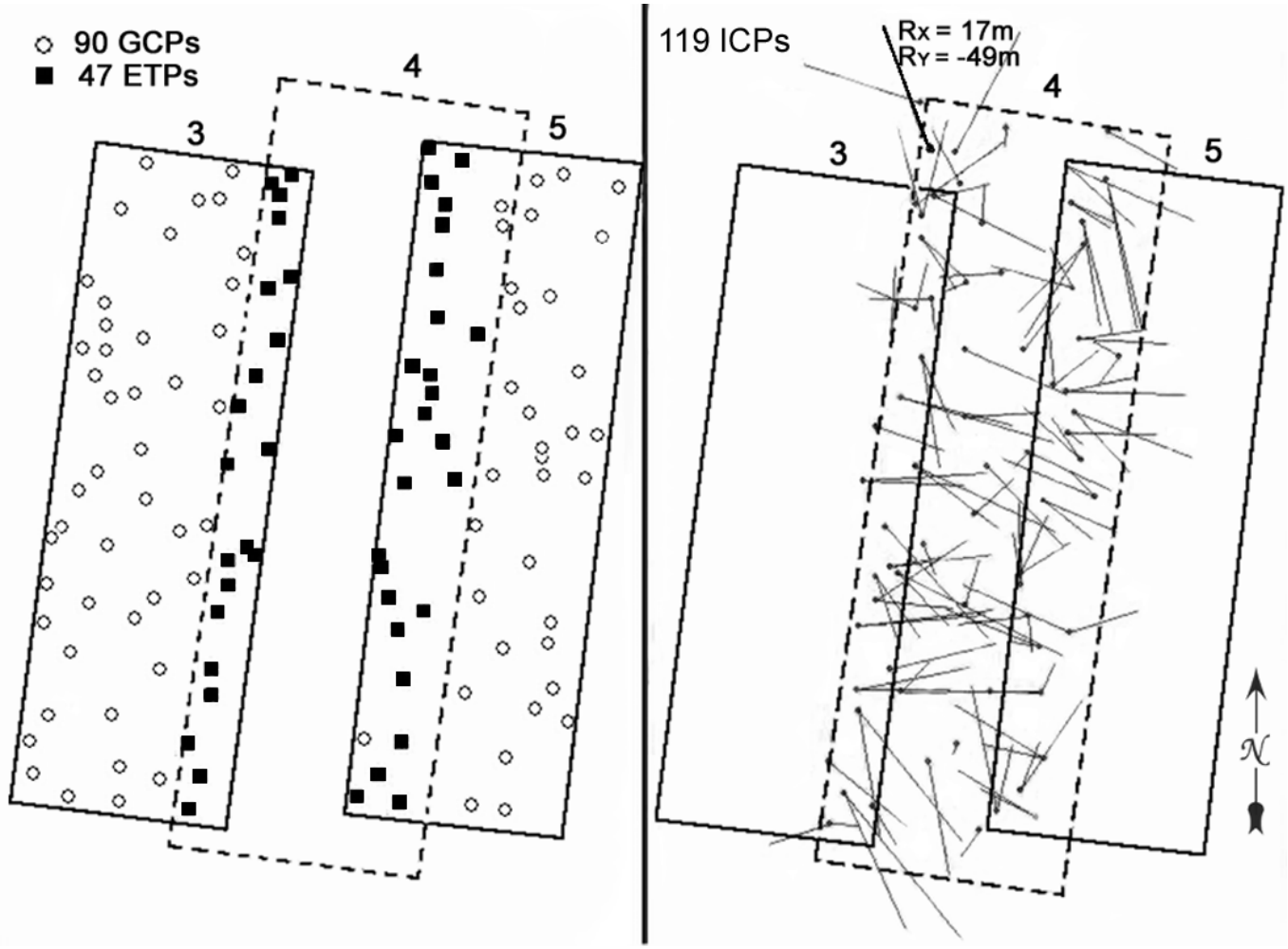

Figure 4: Input data and results of the three-image path block adjustment: GCPs (white circles) and ETPs (black squares) distribution in the left window and the ICP error vectors in the right window. The paths with plain lines are the paths with GCPs. ICP vectors are the differences between the known and the computed cartographic coordinates for each path point. ICPs belonging to more than one path have thus an error vector for each path.

D. GCPs in "checkerboard" for the block

With the *"checkerboard"* configuration, different GCP numbers in the outer paths (1, 5) and the middle path (3) are tested: (i) 54, 62 and 75; (ii) 25, 25 and 25; (iii) 25, 25 and 6; (iv) 10, 10 and 6, respectively (Table IV). For each test, the paths without GCPs were linked with approximately twenty ETPs on each overlap for a total of 88 ETPs. The number of GCPs and ICPs, the RMS residuals for GCPs and the RMS errors for ICPs are synthesised in Table IV. The number of 25 GCPs was chosen as a function of the previous results with the path processing. Since GCPs in the middle path was mandatory, the two last tests were thus chosen to evaluate if the theoretical minimum of six GCPs was enough to stop the error propagation and if the full block can be processed with about the same number of GCPs than an image or a path: the degree of freedom in the least squares adjustment stayed approximately the same due to the 88 ETPs. The two last tests enabled the system robustness and its stability in an operational environment to be evaluated with a minimum requirement of GCPs. For clarity, Fig. 5 only shows the ICP error vectors for the third test.

Table IV: Number of GCPs in *"checkerboard"* distribution (paths 1, 3 and 5) with their RMS residuals (RMS-R), and number of ICPs with their RMS errors (RMS-E) for 5-path block adjustment

Number of GCPs For Paths 1, 3, 5	**RMS-R X (m)**	**RMS-R Y (m)**	**Number of ICPs**	**RMS-E X (m)**	**RMS-E Y (m)**
54, 75, 62	19	17	152	36	26
25, 25, 25	19	15	268	35	27
25, 6, 25	17	15	287	36	26
10, 6, 10	9	5	317	39	29

The general results of Table IV showed good and equivalent results than previous tests considering the checked data quality, but with a slight degradation in the *X*-direction, when the number of GCPs is reduced, due to a smaller degree of freedom in the least squares adjustment: the GCP errors thus propagated more with same-side and weak intersection geometry in the overlaps. However, these results demonstrated a general coherency and confirmed the previous results and their interpretation:

- applicability of the 3-D SAR physical model to block adjustment with reduced number of GCPs;
- stability and robustness of the method regardless of path configurations in the block;
- stability and the robustness of the method regardless of GCP/ETP distributions;
- same number of GCPs (around 25) can be used to process either an image, a path or a block; and
- good relative superposition in the overlap areas; and
- general error of 25-35 m, mainly due to checked data, is quite similar to the error results of one image or path and of THREE-path block adjustment.

ICP error vectors for points belonging to two paths were in the same direction (Fig. 5), demonstrating a good relative superposition between the paths and consequently a good mosaicking. Fig. 5 also demonstrated that there is no general bias or systematic error in the block regardless of path with or without GCPs, and statistical evaluations for each image independently confirmed this last statement. Only a local systematic error in the West direction can be noticed in the overlap between paths 1 and 2. However, the local systematic errors could be also attributed to local systematic errors in some of 42 maps and not necessary to the block adjustment. Consequently, the block adjustment method performed well in terms of relative and absolute accuracy. Since ICP RMS errors (25-30 m cartographic errors) are included in the final RMS errors, the internal accuracy of the block is better (around one SAR resolution cell). Unfortunately, more accurate checked data (better than 10 m) was not available on this study site to quantify the final accuracy.

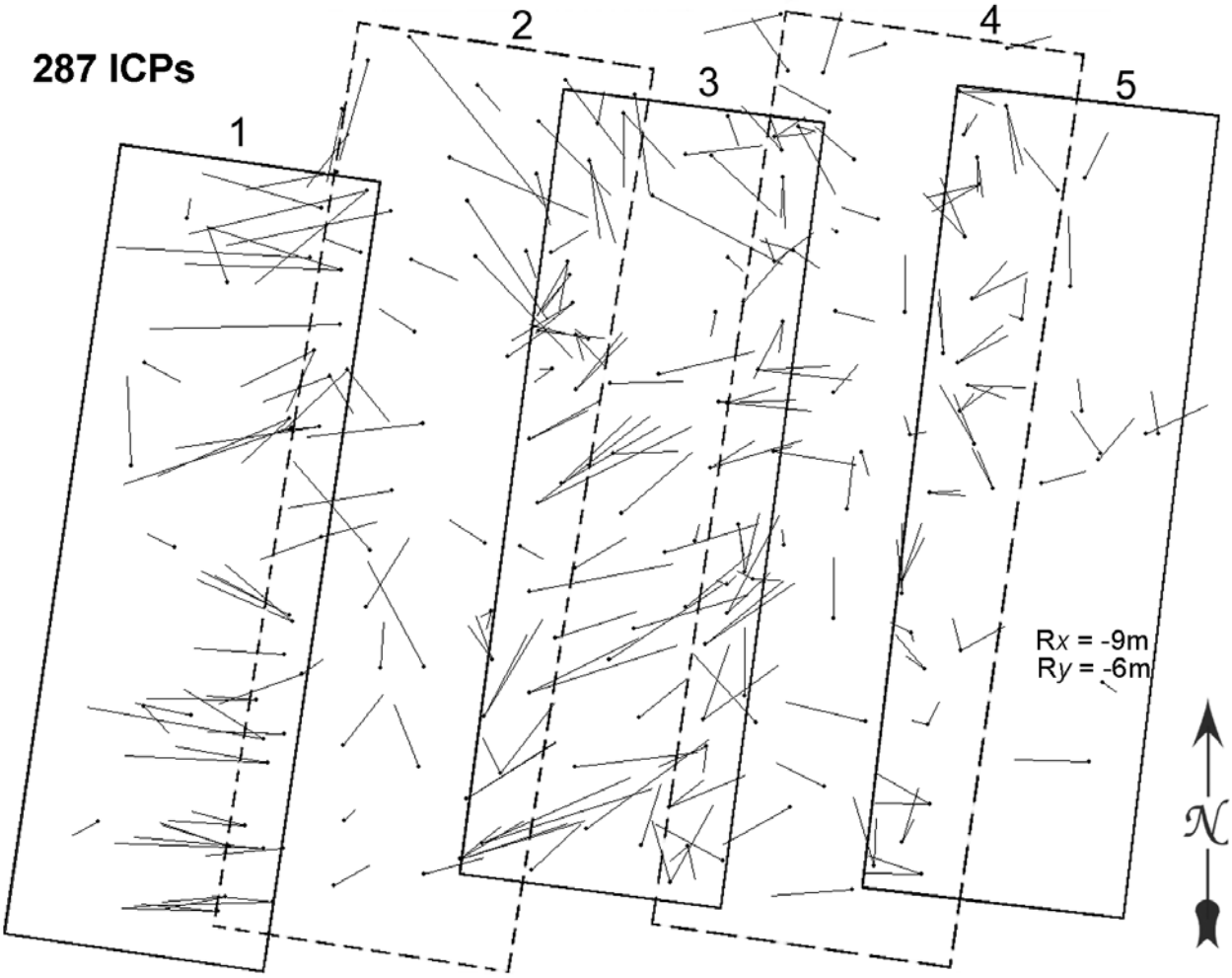

Figure 5: ICP error vectors of the 5-image path block adjustment with *"checkerboard"* configuration: 25 GCPs in the outer paths and 6 GCPs in the middle path. The paths with plain lines are the paths with GCPs. ICP vectors are the differences between the known and the computed cartographic coordinates for each path point. ICPs belonging to more than one path have thus an error vector for each path.

V CONCLUSIONS

When no sufficient ground control is available, a method of spatiotriangulation using an iterative least squares block adjustment to compute CCRS-developed 3-D SAR physical model(s) was tested with 15 RADARSAT-SAR fine mode images acquired over the Canadian Rocky Mountains. The least squares adjustment computed with all GCPs was first tested with independent image, three-image paths and five-path block: the results were similar (around 20- to 25-m RMS residuals). In addition, they were on the same order and even slightly less as the input data errors (image pointing and cartographic). Other test showed that 20 to 25 GCPs in the least squares adjustment was the good compromise for this dataset to not propagate GCP errors in the 3-D SAR physical models. Using this result, path processing and block adjustments were then performed for various GCP distributions and block configurations. In addition to GCPs, ETPs, with a known elevation value, were used in the overlaps because the 6° look-angle difference of overlapping paths is small.

However, when using only GCPs in the outer paths, the adjustment results deteriorated from 25 m in both directions for the three-path block to 270 m in *X* direction for the five-path block. This deterioration is a combination of GCP image pointing and cartographic errors (25-30 m), which propagated through the same-side weak 6°-intersection angle between adjacent F1-F4 paths. Consequently GCP distribution every two paths was the solution with this dataset, and better and consistent results (25-35 m) were achieved using all or a reduced number of GCPs in the outer and middle paths and ETPs in each overlap. Even reducing GCP number to the theoretical minimum (six) in the middle path did not change the results. Finally, the same minimum requirement of GCPs, determined as a function of their accuracy and of the overlap intersection geometry, can be applied for an image, a path or a block if enough ETPs are used to keep the same degree of freedom in the least squares adjustment. This GCP requirement can be carefully applied to other similar dataset, but the more accurate will be the input data and/or the stronger will be the intersection geometry in the overlaps (such as with F1-F5 or S3-S7), the less GCPs will be required.

The tests and results also demonstrated that input GCP errors did not propagate through the physical model, but rather were reflected in RMS residuals/errors. The use of an overabundance of GCPs in the least squares path/block adjustments has reduced or even cancelled the propagation of the input data errors (image pointing and map) in the path/block modelling. Since the combined image pointing and cartographic errors of GCPs were thus included in the final errors results, the internal accuracy of the block should be better (around one SAR resolution cell). Finally, this research study gave a good level of confidence of the applicability and robustness of the CCRS 3-D SAR physical model applied to path/block adjustment with RADARSAT-SAR data, even in operational environment using medium-accurate cartographic sources.

ACKNOWLEDGMENTS

The author thanks Y. Carbonneau (Consultants TGIS inc., Canada) for the block adjustment software package; S. Schulz and. J. Fester (Technische Universität Dresden, Germany) and R. Chénier (Consultants TGIS inc., Canada) for the data processing.

REFERENCES

[1] C. J. Crandall, "Radar mapping in Panama," *Photogrammetric Engineering*, vol. 35, no. 4, pp.1062-1071, July 1969.

[2] L. Azevedo de, "Radar in the Amazon," in *Seventh International Symposium on Remote Sensing of Environment,* Ann Arbor, MI, USA, 9-13 May 1971, pp. 1275-1281.

[3] Ph. Cantou, "French Guiana mapped using ERS-1 radar imagery," (last accessed March 01, 2003; http://www.spotimage.fr/home/appli/apcarto/guiamap/welcome.htm/)

[4] C. Hutton, C. Cloutier, M. Adair and S. Parashar, "RADARSAT-1 Mosaic of Canada," in *22nd Canadian Symposium on Remote Sensing*, Victoria, B.C., Canada, 21-25 August 2000, Available Online: http://www.ccrs.nrcan.gc.ca/ccrs/rd/sci_pub/bibpdf/4809.pdf/, pp. 311-318.

[5] H. Raggam and K.H. Gutjahr, "INSAR Block Parameter Adjustment," in *3rd European Conference on SAR,* Munich, Germany, 23-25 May, 2000, pp. 493-496.

[6] Y. Belgued, S. Goze, J.-P. Planès and Ph. Marthon, "Geometrical Block Adjustment of Multi-Sensor Radar Images," *in EARSeL Workshop: Fusion of Earth Data,* Sophia-Antipolis, France, January 26-28, 2000, pp. 11-16.

[7] Th. Toutin, Y. Carbonneau and L. St-Laurent, An Integrated Method to Rectify Airborne Radar Imagery Using DEM, *Photogrammetric Engineering and Remote Sensing*, vol. 58, no. 4, pp. 417-422, 1992.

[8] Th. Toutin, «Evaluation de la précision géométrique des images de RADARSAT,» *Canadian Journal of Remote Sensing,* vol. 23, no. 1, pp. 80-88, Available Online: http://www.ccrs.nrcan.gc.ca/ccrs/rd/sci_pub/bibpdf/3277.pdf/, Jan. 1998.

[9] Th. Toutin, "Evaluation of radargrammetric DEM from RADARSAT images in high relief areas," *IEEE Trans. on Geoscience and Remote Sensing,* vol. 38, no. 2, pp. 782-7898, Available Online: http://www.ccrs.nrcan.gc.ca/ccrs/rd/sci_pub/bibpdf/4752.pdf/, Feb. 2000.

[10] N. Denyer, R.K. Raney and N. Shepperd, "The RADARSAT SAR data processing facility," *Canadian Journal of Remote Sensing*, vol. 19, no. 4, pp. 311-316, Dec. 1993.

[11] S. Sylvander, D. Cousson et P. Gigord, «Etude des performances géométriques de Radarsat,» *Bulletin de la Société Française de Photogrammétrie et de Télédétection*, vol. 148, no. 4, pp. 57-65, 1997.